RESEARCH ARTICLE | FEBRUARY 22 2024

# Wire texture C-axis distribution of strontium ferrite/PA-12 extruded filament

Special Collection: 68th Annual Conference on Magnetism and Magnetic Materials

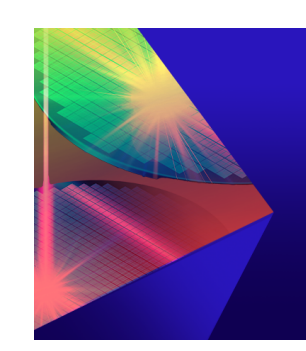
Gabriela Espinosa-Rodriguez ■ ⑩ ; Oluwasola Arigbabowo ⑩ ; Jonathan Alvarado; Jitendra Tate ⑩ ; Wilhelmus J. Geerts ⑪



AIP Advances 14, 025245 (2024) https://doi.org/10.1063/9.0000701







# **AIP Advances**

Special Topic: Novel Applications of Focused Ion Beams — Beyond Milling

**Submit Today** 





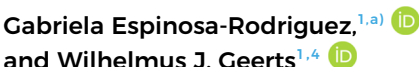
# Wire texture C-axis distribution of strontium ferrite/PA-12 extruded filament

Cite as: AIP Advances 14, 025245 (2024); doi: 10.1063/9.0000701 Submitted: 2 October 2023 • Accepted: 25 December 2023 • Published Online: 22 February 2024











Gabriela Espinosa-Rodriguez, 1, a) Doluwasola Arigbabowo, 2 Donathan Alvarado, 3 Jitendra Tate, 2, 4 Donathan Alvarado, 3 Jitendra Tate, 3 Donathan Alvarado, 3 Donathan Alva



# **AFFILIATIONS**

- Department of Physics, Texas State University, San Marcos, Texas 78666, USA
- <sup>2</sup>Materials Science, Engineering, and Commercialization, Texas State University, San Marcos, Texas 78666, USA
- <sup>3</sup>University of Texas Rio Grande Valley, Edinburg, Texas 78539, USA
- Mechanical and Manufacturing Engineering, Texas State University, San Marcos, Texas 78666, USA

Note: This paper was presented at the 68th Annual Conference on Magnetism and Magnetic Materials.

<sup>a)</sup>Author to whom correspondence should be addressed: glynnette@txstate.edu

# **ABSTRACT**

The magnetic anisotropy of strontium ferrite (SF)/PA12 filament, a popular hard magnetic ferrimagnetic composites that is used for 3Dprinting of permanent magnets, is studied by vibrating sample magnetometry. The studied filaments have a composition of SF/PA-12 thermoplastic composite with a 40% wt. ratio of SF. SF particles are non-spherical platelets with an average diameter of 1.3 um and a diameter to thickness ratio of 3. Filaments are produced by a twin-screw extruder and have a diameter of 1.5 mm. SEM images show that the SF particles are homogeneously distributed through the filament. VSM measurements on different parts of the filaments show that the outer part of the cylindrical filament has a higher anisotropy, and the core is mostly isotropic. This conclusion is consistent with computational work by others which suggest that particle alignment predominantly takes place near the walls of the extruder die where shear flow is maximum. Additional hysteresis curve measurement of the outer cylindrical part of the filament parallel to the r and  $\phi$  directions indicates that the squareness of the hysteresis curve (S) is larger in the r-direction. This indicates that the outer surface of the filament has a strong easy axis in the r-direction. We conclude that the SF platelets line up parallel to the walls of the extrusion die.

© 2024 Author(s). All article content, except where otherwise noted, is licensed under a Creative Commons Attribution (CC BY) license (http://creativecommons.org/licenses/by/4.0/). https://doi.org/10.1063/9.0000701

# I. INTRODUCTION

3D printing of magnetic composites has been explored for fast prototyping because of its cost-effectiveness and production rate. Recently one started exploring the use of a magnetic field during the 3D printing process to induce a magnetic anisotropy in the 3D printed materials. For permanent magnets, the anisotropic arrangement is often preferred since it has a stronger magnetization than an isotropic one, which is due to the organized structure of an anisotropic material. Isotropic materials have the same topography, but they are randomly orientated.

The first Magnetic Field Assisted Additive Manufacturing (MFAAM) experiments were done by printing on permanent magnets placed on the print bed of an FDM printer.1 Others used an electromagnet<sup>2,3</sup> or a permanent magnetic field fixture<sup>4</sup> on the 3D

printer-head. MFAAM has been shown to enhance material properties such as susceptibility,<sup>5</sup> remanence,<sup>6</sup> and yielding strength. It has also paved a path to new manufacturing method that allows to realize materials and devices whose magnetic anisotropy axis vary with position leading to magnets that can lift more, printable flux-guides for wearable electronics, or Halbach cylinders with very homogeneous fields that one day will replace the superconducting magnets in MRI equipment realizing a portable version of the diagnosis tool.

Except for an external magnetic field also a shear flow can affect the orientation of non-spherical particles in a suspension.<sup>7</sup> Flow induced magnetic anisotropy was observed in freely extruded strontium-ferrite (SF) PA-12 filaments<sup>10</sup> and recently also in 3D printed samples of the same material.<sup>11</sup> These SF particles are non-spherical (oblate spheroids or platelets), so their alignment is

20 August 2024 18:51:08

affected by the variation of the velocity of the fluid in the extrusion die, the shear flow. <sup>12</sup> In this paper we explore the distribution of the orientation of SF platelets through an extruded SF/PA-12 filament to better understand the origin of the flow induced anisotropy. This is relevant for 3D printing of SF/PA-12 magnetic composites and might help with the further development of Flow Assisted Additive Manufacturing (FAAM).

# II. EXPERIMENTAL PROCEDURE AND METHODOLOGY

Experiments were done on 40 wt. % SF/AP-12 filaments. 6,10 Vestosint® 3D Z2773 PA-12 from Evonik was used for the base of magnetic composite and OP-71 powder from Dowa Electronics Materials Co. for the SF particles. This is a thermoplastic polymer known as nylon. It acts as a filler between the SF platelets and as an adhesive to keep the SF platelets together. The filaments were extruded in a Thermo Fisher Process 11 Co-rotating Twin Screw Extruder. More details on the manufacturing process are provided in Ref. 4. The SF particles were single domain with an average size of 1.3 um. SEM images (Fig. 1) show that the SF particles are platelets with a diameter to thickness ratio of approximately three. No clustering of particles was observed in material extruded in zero field for the hollow cylinder [Fig. 1(a)] and the core [Fig. 1(b)]. For this material, the crystal anisotropy of the individual particles is the most important contributor to the sample's magnetic anisotropy. This type of anisotropy is more focused on the platelets or individual particles of the magnetic composite than the general shape of the sample. Because of the low packing fraction (8 vol. %) sample shape anisotropy can be ignored in this paper. The crystal anisotropy is caused by spin-orbit interaction and crystal electric field. This effect couples the direction of the magnetic moment in the material to the crystal structure. If the magnetic moment is along the c-axis of the SrFe<sub>12</sub>O<sub>19</sub> hexagonal ferrite platelets, the magnetic energy is lowest. The single crystalline platelets have an easy axis, the axis that is easiest to saturate, perpendicular to their surface [Fig. 2(a)]

The SF/PA-12 filaments have an easy plane perpendicular to the filament's cylindrical axis. <sup>10</sup> Two hypotheses were drawn on the orientation the SF platelets would take as they tumble or spin down the extrusion die in the molten PA-12. The first one is that the ferromagnetic platelets would arrange themselves with their easy axis perpendicular to the cylindrical surface of the filament Fig. 2(b). The other possible orientation for the platelets would be that they arrange

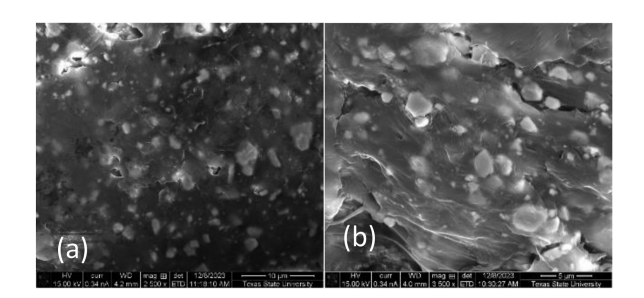


**FIG. 1.** SEM Images of the outer surface of the hollow cylinder and core. (a) hollow cylinder surface at 10  $\mu$ m. (b) core surface at 5  $\mu$ m.

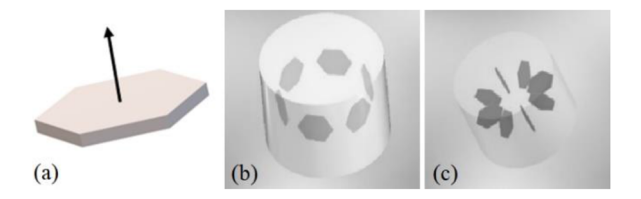


**FIG. 2.** (a) Platelet easy axis perpendicular to the surface (b) the easy axis would be facing the outer shell and (c) the platelets would be parallel to each other.

themselves parallel to each other, so their easy axis is pointing in the filament's f direction Fig. 2(c). Note that both configurations would result in the observed easy plane perpendicular to the filament's cylindrical axis.

To determine what part of the filament is anisotropic and what part is isotropic, samples were cut from a 1.5 mm diameter filament using a knife and a dissecting tool. First the filament was cleaned with a Kim wipe and IPA to remove any impurities on its surface. Then a 1.5 mm long disk was cut from the filament. With a dissecting tool the center of the disk (1 mm diameter) was extracted. This process is sketched in Figs. 3(a) and 3(b). This process creates two samples here referred to as the core and the donut sample. A Cahn C30 microgram scale was used to determine the mass of each sample and a Hirox digital microscope to obtain the sample's dimensions. Lastly, the samples were glued to 8 mm round cover glass slides.

To determine the filaments texture [Figs. 1(b) and 1(c)] a third type sample was prepared. The same process as described above was used to determine another hollow sample. Before mounting the sample on a glass slide though, an incision was made on one side of the donut sample along its cylindrical axis. The donut sample was opened, and a clamp was used to flatten it on a firm surface [Figs. 3(c) and 3(d)]. Finally, the flattened sample was glued to an 8 mm round cover glass slide.

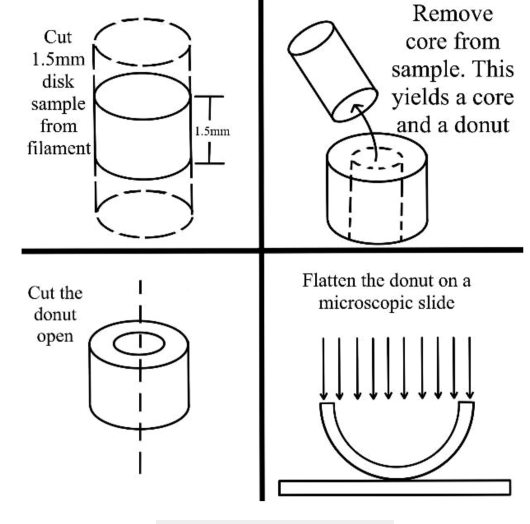


FIG. 3. Sample preparation.

The museum wax was used to load the prepared samples on a perpendicular and transverse rod. This creates a large adhesion between the cover slide and the rod that will prevent the sample from falling during the data gathering.

Magnetic hysteresis curves were measured for different field directions using a MicroSense EZ9 vibrating sample magnetometer (VSM) using sweep mode (200 Oe/sec). The VSM measurement principle is based on Faraday's law of induction where the head of the VSM vibrates the sample between the pickup coils. The sample's magnetic field induces an electric field in the pickup coils resulting in an induced voltage that is measured by a locking amplifier. This signal is proportional to the sample's magnetic dipole moment. A large electromagnet applies an external magnetic field ranging from -22000 to  $22\,000$  Oe to the sample.

Hysteresis curves were measured for two different field angles. For the core and hollow cylinder samples, the hysteresis was measured for H parallel to the r-direction and for H parallel to the cylindrical long axis of the filament. For the flat sample, the hysteresis curves were taken for H parallel to the f direction and H parallel to the r-direction.

# III. RESULTS

The measured hysteresis curves were corrected for the image effect and the field lag and the squareness ( $S = M_r/M_s$ ) and  $M_s$  were determined from these corrected hysteresis curves. Data for typical hollow cylinder and core samples is summarized in Table I below. The squareness ( $S = M_r/M_s$ ) of the measured hysteresis curves parallel to the filament's z-axis ( $S_z$ ) and r-axis ( $S_r$ ) are compared. It was found consistently that the  $S_r/S_z$  is larger for the hollow cylinder than for the core samples as seen in Table I. So, the core samples are more isotropic, and the donut samples have a larger anisotropy. A more elaborate comparison that also corrects for the demagnetizing field shows the same trend. No significant difference in magnetic moment per unit mass was observed between the core samples and the hollow cylinder.

The hysteresis curves of the flattened sample H parallel to  $\phi$  (red dotted line) and H parallel to r-direction (purple line) are shown

**TABLE I.** Magnetic anisotropy samples. The density of the sample can be seen on Table II.

	H//to r-direction		H//to cylinder. Axis	
Sample ID1.00MM 0.5-1	S <sub>r</sub>	M <sub>S</sub> (emu/g)	Sz	M <sub>S</sub> (emu/g)
Hollow cylinder Core	0.59 0.57	31.40 31.23	0.39 0.42	30.41 31.76

TABLE II. Density of the hollow cylinder and core.

Sample ID1.00MM 0.5-1	Density (g/cm <sup>3</sup> )
Hollow cylinder	1.7 ± 0.15
Core	$2.1 \pm 0.15$

# Flattened donut sample

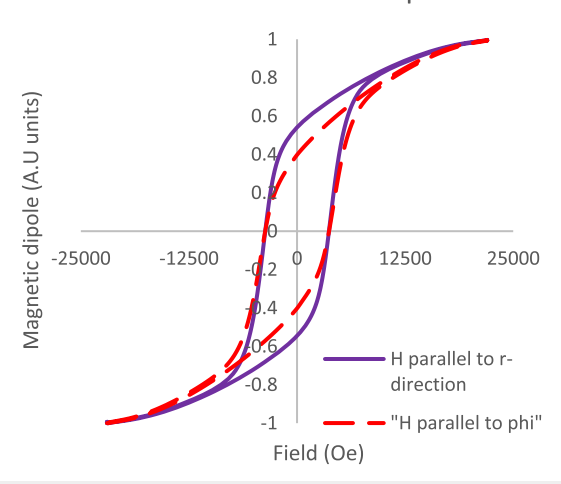


**FIG. 4.** Hysteresis curves parallel to  $\varphi$  direction (dashed red) and parallel to r direction (solid purple).

below in Fig. 4. We can see that the S is low when H is parallel to f and high when and H is parallel to the r-direction. This indicates that the r-direction is an easy axis of the magnetic anisotropy. This confirms that the c-axis of the platelets are organized perpendicular to the surface of the filament as shown in Fig. 2(b).

# IV. CONCLUSION

As a result, it was concluded that the outer surface of the filament is more anisotropic than the core Table I. In the light of this information another experiment was done to determinate the crystal anisotropy it was found that S is higher when H is parallel to the r-direction as seen on Fig. 4 showing that platelets are perpendicular to the surface correlating with the model on Fig. 2(c). These results match with what the computational group previously predicted, which indicated that the extruded filaments have a higher anisotropy along the outer surface of the filament. This research is beneficial to the FAAM field since it provides an understanding of how flow influences magnetic anisotropy in FFF. Understanding this is crucial to use FAAM to 3D print anisotropic hard magnets. If we know how the alignments work, we can manipulate and improve upon the printing process, important for a wide-scale application in an industrial setting.

# **ACKNOWLEDGMENTS**

Great gratitude to the master's students from the Fall-2022 PHYS5304 class Arjun Sapkota, Sujan Pyakurel, Nicholas Moore, Sunil Adhikari, Rajendra Rai, Sarah Smith, Ujjwal Dhakal, Pukar Sendai at Texas State University for being the root of inspiration towards this experiment.

This work was supported in part by NSF (NATIONAL SCIENCE FOUNDATION) through DMR- MRI Grant under awards 2216440.

#### **AUTHOR DECLARATIONS**

# **Conflict of Interest**

The authors have no conflicts to disclose.

# **Author Contributions**

Gabriela Espinosa-Rodriguez: Conceptualization (equal); Data curation (equal); Formal analysis (equal); Investigation (equal); Methodology (equal); Project administration (equal); Visualization (equal); Writing – original draft (equal); Writing – review & editing (equal). Oluwasola Arigbabowo: Conceptualization (equal); Writing – review & editing (equal). Jonathan Alvarado: Data curation (supporting); Writing – review & editing (equal). Jitendra Tate: Investigation (equal); Resources (lead); Supervision (equal); Writing – review & editing (equal). Wilhelmus J. Geerts: Conceptualization (equal); Formal analysis (equal); Funding acquisition (equal); Investigation (equal); Methodology (equal); Project administration (equal); Resources (equal); Supervision (equal); Validation (equal); Visualization (equal); Writing – review & editing (equal).

#### **DATA AVAILABILITY**

The data that support the findings of this study are available from the corresponding author upon reasonable request.

# **REFERENCES**

<sup>1</sup>C. Huber, S. Cano, I. Teliban, S. Schuschnigg, M. Groenefeld, and D. Suess, "Polymer-bonded anisotropic SrFe<sub>12</sub>O<sub>19</sub> filaments for fused filament fabrication," Journal of Applied Physics **127**, 063904 (2020).

- <sup>2</sup>A. Sarkar, M. P. Paranthaman, and I. C. Nlebedim, "*In-situ* magnetic alignment model for additive manufacturing of anisotropic bonded magnets," Additive Manufacturing **46**, 102096 (2021).
- $^{\mathbf{3}}\text{M}.$  Ho, "Magnetic 3D printing of hexaferrite material," Dissertation (UCLA, 2019).
- <sup>4</sup>M. Suppan, C. Huber, K. Mathauer, C. Abert, F. Brucker, J. Gonzalez-Gutierrez, S. Schuschnigg, M. Groenefeld, I. Teliban, S. Kobe, B. Saje, and D. Suess, "In-situ alignment of 3D printed anisotropic hard magnets," Scientific Reports 12, 17590 (2022).
- <sup>5</sup>L. Henderson, S. Zamora, T. N. Ahmed, C. Belduque, J. Tate, M. Yihong Chen, and W. J. Geerts, "Altering magnetic properties of Iron filament PLA using magnetic field assisted additive manufacturing (MFAAM)," Journal of Magnetism and Magnetic Materials 538, 168320 (2021).
- <sup>6</sup>C. Belduque, R. Robinson, A. Medina, T. Ahmed, R. Kala, W. Geerts, and J. Tate, "Magnetic and mechanical characterization of additive manufactured strontium ferrite/polyamide 12 composites using twin-screw and single-screw extrusion," in SAMPE 2021 Conference Proceedings, Long Beach, CA, 24–27 May 2021.
- <sup>7</sup>Z. Wang and D. E. Smith, "Finite element modeling of fully-coupled flow/fiber-orientation effects in polymer composite deposition additive manufacturing nozzle-extrudate flow," Compos. Part B Eng. 219, 108811 (2021).
- <sup>8</sup>S. Yashiro, H. Sasaki, and Y. Sakaida, "Particle simulation for predicting fiber motion in injection molding of short-fiber-reinforced composites," Composites Part A: Applied Science and Manufacturing 43(10), 1754–1764 (2012).
- <sup>9</sup>B. Brenken, E. Barocio, A. Favaloro, V. Kunc, and R. B. Pipes, "Fused filament fabrication of fiber-reinforced polymers: A review," Additive Manufacturing **21**(2010), 1 (2018).
- <sup>10</sup>T. N. Ahmed, M. C. Belduque, D. C. Binod, J. S. Tate, and W. J. Geerts, AIP Advances 11(1–5), 015048 (2021).
- <sup>11</sup>A. Sapkota, L. Rodriguez, D. C. Binod, K. Dieckow, C. Q. Howlader, W. J. Geerts, and J. Tate, "On the origin of systematic errors in VSM torque curves," AIP Adv. Fall (2023) submitted to.
- <sup>12</sup>M. Trebbin, D. Steinhauser, J. Perlich, A. Buffet, S. V. Roth, W. Zimmermann, J. Thiele, and S. Forster, Proc. Natl. Acad. Sci. U. S. A 110(17), 6706–6711 (2013).